EUROPEAN ORGANIZATION FOR NUCLEAR RESEARCH

ISR-TH/69-8

MAGNETIC FIELD AND GEOMETRY OF THE ISR

by

K. Hübner, E. Keil and L. Resegotti

Geneva - 10 March, 1969

PS/7088

SUMMARY

The methods and data employed in the determination of the gradient of the ISR magnets and of the ISR geometry are described. In particular, Part I contains the description of the hard edge approximation work on which all the designs were based. Part II describes work using a smooth field table and tracking trajectories through it which was mainly done for checking the approximate work of Part I. Good agreement between the two approaches was obtained.

Part I. Hard edge approximation

I.1 Introduction and Definitions

The main ISR magnet of each ring consists of 192 rectangular magnet blocks which are arranged as follows:

40 short F units composed of one block
32 short D units composed of one block
28 long F units composed of two blocks
32 long D units composed of two blocks.

The expression "rectangular magnet block" describes its geometrical shape and - at the same time - indicates some of its consequences.

i) Since a rectangular magnet block does not follow the curvature of the equilibrium orbit the latter is not geometrically distinguished from any other orbit through the magnet and must hence be defined explicitly (I.3).

ii) Since the end faces of the magnet are parallel to each other they are not perpendicular to the equilibrium orbit and hence additional focusing occurs at the magnet ends which must be taken into account (I.5).

In the hard-edge approximation the smooth magnetic field and gradient at the ends of the magnet blocks are replaced by magnetic fields and gradients which are piecewise constant and abruptly change at the edges in such a way that the integrals of the smooth fields and of the hard-edge approximation are equal.

We use the coordinate system shown in Fig. 1. We first define the effective bending power of half a magnet block by the equation:

$$B(x,o)\, L_B(x) = \int_o^{s_n(x)} B(x,s)\, ds \qquad (1)$$

L_B is the effective length for field of half a block. The limit of the integration s_n is conveniently chosen far away from the magnet block such that the magnetic field vanishes there. This is possible for the short units.

The two blocks of a long unit are so close together that their stray fields interfere. In this case, the integration limit occurs in an azimuthal position where the magnetic field does not vanish, and becomes itself a function of x, since there is a small angle between the two blocks of a long unit.

Differentiating (1) with respect to x gives us the effective focusing power of half a magnet block:

$$\frac{d}{dx}\left[B(x,o)\, L_B(x)\right] = \frac{dB}{dx}(x,o)\, L_G(x)$$

$$= \int_o^{s_n(x)} \frac{\partial B(x,s)}{\partial x}\, ds + B(x,s_n(x))\, \frac{ds_n(x)}{dx} \qquad (2)$$

L_G is the effective length for gradient of half a block. Only the first term on the right hand side remains when the limits of integration are in a field free region.

For practical purposes it is more convenient to define length corrections ℓ_B and ℓ_G for each end of a magnet block such that

$$\ell_B(x) = L_B(x) - \tfrac{1}{2} L_n \qquad (3)$$

$$\ell_G(x) = L_G(x) - \tfrac{1}{2} L_n \qquad (4)$$

L_n is the physical length of a magnet block.

I.2 Compilation of magnet data

Table 1 is an abstract of the ISR parameter list[1] giving the relevant magnet parameters. There are three different kinds of effective lengths ℓ_B and ℓ_G for the following ends of magnet blocks:

i) the end with coil connections facing a straight section
ii) the end without coil connections facing a straight section
iii) the end facing the other block of a long magnet unit.

The coil connections of all magnet units are at the counterclockwise end. The effective lengths L_B and L_G of all kinds of blocks are then sums of the appropriate ℓ_B's and ℓ_G's and L_n.

I.3 Equilibrium Orbit in Individual Magnet Blocks

I.3.1 Relative Position of Equilibrium Orbit and Magnet Centre Line

In a rectangular magnet unit, the magnetic field has the following form:

$$B(x,o) = B(o,o) + x \left.\frac{dB}{dx}\right|_{o,o} + \frac{x^2}{2} \left.\frac{d^2B}{dx^2}\right|_{o,o} \qquad (5)$$

and a gradient

$$B'(x,o) = \left.\frac{dB}{dx}\right|_{o,o} + x \left.\frac{d^2B}{dx^2}\right|_{o,o} \qquad (6)$$

Since the equilibrium orbit will be curved it will not pass through the same magnetic field along the whole magnet block. We shall first calculate how the equilibrium orbit must pass through the field (5) in order to undergo the same total deflection as in a curved magnet of the same length and field B_o.

We approximate the equilibrium orbit by a parabola starting at a distance x_o from the magnet centre line in the middle of the block as shown in Fig. 1:

$$x = x_o + \frac{s^2}{2\rho} \qquad (7)$$

The following equation should hold with the integration path c extended over half a magnet block:

$$B_o L = \int_c B(x)\, ds \qquad (8)$$

L is the abbreviation for $L = L_n/2 + \ell_B$.
Substituting (5) into (8) and performing some algebra yields the following solution

$$x_o = \frac{-\frac{n}{\rho} + \frac{L^2}{3!\rho}\,\frac{n'}{\rho} \pm \frac{n}{\rho}\left(1 + \frac{14}{180}\,\frac{L^4}{\rho^2}\left(\frac{n'}{n}\right)^2\right)^{\frac{1}{2}}}{\frac{n'}{\rho}} \qquad (9)$$

When doing the integral in (8) we neglect the small angle between the trajectory and the z axis and integrate with respect to z. The

resulting small error is taken care of later on by applying a "curvature correction" (I.3.2).

Developing the square root in (9) we find

$$x_o = \frac{L^2}{6\rho} + \frac{7}{180}\,\frac{L^4}{\rho^2}\left(\frac{n'}{n}\right) \tag{10}$$

The following shorthand was used

$$\frac{n}{\rho} = -\frac{1}{B_o}\,\frac{dB}{dx} \tag{11}$$

$$\frac{n'}{\rho} = -\frac{1}{B_o}\,\frac{d^2B}{dx^2} \tag{12}$$

In the constant gradient case with $n' = 0$, x_o is just 1/3 of the sagitta of the particle trajectory. In the case of the ISR the correction term for $n' \neq 0$ is 300 times smaller than the first term.

A similar integration may be performed to find the total focusing power of a straight magnet

$$\int_c \frac{dB}{dx}\,ds \tag{13}$$

This becomes by substituting (6) into (13) and doing some algebra, again integrating with respect to z:

$$\frac{\int_c \frac{dB}{dx}\,ds}{\frac{dB}{dx}\,L} = 1 + \frac{7}{180}\,\frac{L^4}{\rho^2}\left(\frac{n'}{n}\right)^2 \tag{14}$$

Here L is an abbreviation for $L = L_n/2 + \ell_G$. Inserting ISR parameters into (14) shows that the change of focusing power due to the assumed rectangular magnet blocks is completely negligible.

On the basis of (10) it was decided to put the equilibrium orbit into all magnet blocks in the manner shown in Fig. 1. The equilibrium orbit crosses the effective border of the magnetic field at a distance $a = -7.2$ mm inside the magnet centre line.

I.3.2 Effective lengths of the magnet blocks

Knowing the position of the equilibrium orbit in the magnet blocks permits an accurate calculation of their effective lengths L_B and L_G. We have to take into account the following length modifications:

i) Effective length corrections ℓ_B or ℓ_G.

ii) Exit corrections, add $a \frac{\partial L_B}{\partial x}$ or $a \frac{\partial L_G}{\partial x}$.

iii) Curvature correction, multiply by $\frac{\phi}{2} / \sin \frac{\phi}{2}$.

The second correction is due to the radial variation of the effective lengths ℓ_B and ℓ_G which must be taken at the radial position where the equilibrium orbit actually crosses the end of the magnet. The third correction is necessary because we integrate (8) and (13) with respect to z rather than along the trajectory s.
The formula for calculating the bending length L'_B of a magnet block becomes:

$$L'_B = \left[L_n + \ell_{B1} + \ell_{B2} + a \left(\frac{\partial L_B}{\partial x} \right)_1 + a \left(\frac{\partial L_B}{\partial x} \right)_2 \right] \frac{\phi/2}{\sin \phi/2} \qquad (15)$$

The corresponding formula for the focusing length L'_G is:

$$L'_G = \left[L_n + \ell_{G1} + \ell_{G2} + a\left(\frac{\partial L_G}{\partial x}\right)_1 + a\left(\frac{\partial L_G}{\partial x}\right)_2 \right] \frac{\phi/2}{\sin\phi/2} \qquad (16)$$

The indices 1 and 2 refer to the two ends of the magnet block. An approximate value must be used for ϕ at this stage. This is sufficient since the curvature correction is small. The bending lengths L'_B and the focusing lengths L'_G were calculated from the data shown in Tab. 1; they are summarized in Tab. 2.

I.3.3 Bending Angles of the Blocks

The bending angles can be calculated using the following argument. The total bending angle in a superperiod is $\pi/2$, and the total effective length of the magnets in a superperiod Σ can be calculated by multiplying their lengths given in Tab. 2 by their number. We find:

$$\Sigma = 123.44808 \text{ m} \qquad (17)$$

and hence

$$\rho = \frac{\Sigma}{\pi/2} = 78.5895 \text{ m} \qquad (18)$$

The bending angle ϕ is then simply:

$$\phi = \frac{L_B}{\rho}$$

The results are also shown in Tab. 2.

I.3.4 Effective Lengths of the Straight Sections

The physical length of the straight sections in the ISR is defined as the distance between the two points where the centre lines of two neighbouring magnet blocks cross their end faces. This is shown in Fig. 1. The total length of the magnet blocks and straight sections is chosen such that the equilibrium orbit has the correct

TAB. 1. MAGNET PARAMETERS.

MAXIMUM FIELD AT EQUILIBRIUM ORBIT	BZERO	1.2	T
CORE LENGTH OF A LONG MAGNET UNIT	L(L)	5.030	M
CORE LENGTH OF A SHORT MAGNET UNIT	L(S)	2.440	M
SPACE BETWEEN THE TWO BLOCKS IN A LONG UNIT	A1	0.150	M
BENDING RADIUS	RHO	78.5895	M
BENDING ANGLE IN CONNECTION HALF OF LONG F UNIT		0.032606057	RAD
BENDING ANGLE IN CONNECTION HALF OF LONG D UNIT		0.032572972	RAD
BENDING ANGLE IN FREE HALF OF LONG F UNIT		0.032579335	RAD
BENDING ANGLE IN FREE HALF OF LONG D UNIT		0.032546250	RAD
BENDING ANGLE IN SHORT F UNIT		0.032995694	RAD
BENDING ANGLE IN SHORT D UNIT		0.032948484	RAD
PROFILE PARAMETER IN F MAGNETS	N/RHO(F)	-3.133	1/M
PROFILE PARAMETER IN D MAGNETS	N/RHO(D)	+3.018	1/M
RADIAL DERIVATIVE OF F PROFILE PARAMETER	N'/RHO(F)	-1.940	1/M*M
RADIAL DERIVATIVE OF D PROFILE PARAMETER	N'/RHO(D)	+1.496	1/M*M

ASSUMED EFFECTIVE LENGTHS	FIELD	GRADIENT	
CONNECTION END OF F BLOCK	0.0766	0.0329	M
CONNECTION END OF D BLOCK	0.0766	0.0335	M
FREE END OF F BLOCK	0.0745	0.0334	M
FREE END OF D BLOCK	0.0745	0.0339	M
HALF JUNCTION OF LONG F UNIT	0.0445	0.0297	M
HALF JUNCTION OF LONG D UNIT	0.0445	0.0257	M

ASSUMED RADIAL DERIVATIVES OF EFFECTIVE LENGTH.	FIELD	GRADIENT
AVERAGE OF CONNECTION AND FREE END OF F BLOCK	-0.132	-0.228
AVERAGE OF CONNECTION AND FREE END OF D BLOCK	+0.126	+0.228
HALF JUNCTION OF LONG F UNIT	-0.046	-0.099
HALF JUNCTION OF LONG D UNIT	+0.057	+0.123

Tab. 2. Effective Lengths and Bending Angles of Magnet Blocks

Type	L_B' [m]	L_G' [m]	ϕ [rad]
Block of long F unit with coil connection	2.56249	2.5051	0.032606057
Block of long F unit without coil connection	2.56039	2.5056	0.032579335
Block of long D unit with coil connection	2.55989	2.4968	0.032572972
Block of long D unit without coil connection	2.55779	2.4972	0.032546250
Short F unit	2.59312	2.5097	0.032995694
Short D unit	2.58941	2.5042	0.032948484

circumference (I.4.1). The effective length of a straight section is smaller than their physical length for two reasons:

i) The effective length added to the neighbouring magnet blocks must be subtracted.

ii) There is an angle between the magnet end faces and the equilibrium orbit crosses the straight section at a distance $a = -7.2$ mm.

We have the following expression for the "effective focusing length" of a straight section:

$$L_{SG} = L_S - \ell_{G1} - \ell_{G2} - a\left(\frac{\partial L_G}{\partial x}\right)_1 - a\left(\frac{\partial L_G}{\partial x}\right)_2 + \frac{a}{2}(\phi_1 + \phi_2) \quad (20)$$

L_S is the physical length of a straight section. The indices 1 and 2 refer to the magnet ends on either side of the straight section. A comparison between the physical lengths and the effective lengths of the straight sections is shown in Tab. 3.

Tab. 3. Straight Section Lengths

Type		L_S [m]	L_{SG} [m]
A0,	coil connection on F block no connection on D block	1.63	1.5630
A0,	coil connection on D block no connection on F block	1.63	1.5629
A1,	between F blocks	0.15	0.0889
A1,	between D blocks	0.15	0.1001
A2		16.783	16.7132
A3		2.000	1.9356
A4		13.0042	12.9344
A5		2.000	1.9356
A6		9.600	9.5302

I.4 ISR Geometry

I.4.1 The circumference of the ISR

The circumference of the ISR equilibrium orbit is determined by the requirement that within tolerances given below the circumference of the ISR injection orbit be equal to 3/2 of the circumference of the PS ejection orbit.

It turns out that the circumference of the ISR injection orbit is not a unique number. Rather, a range of values is required depending on the following operational parameters:

i) the size of the injected beam
ii) the closed orbit distortions in the ISR
iii) the Terwilliger scheme.

The necessary range to cover the operation with and without the Terwilliger scheme with the present ISR beam size is

$$\frac{\Delta R}{R} = 1.14 \times 10^{-4} \qquad (21)$$

If two-turn injection into the ISR from booster + PS is to be included the required range increases to

$$\frac{\Delta R}{R} = 1.88 \times 10^{-4} \qquad (22)$$

If there is no frequency difference between the ISR and the PS, the range of ejection orbit radius is also given by (21) and (22).

The following equation must hold

$$\frac{3}{2} R^{e}_{PS} = R^{i}_{ISR} \qquad (23)$$

where the index e indicates ejection, and i indicates injection. To find the radius R_{ISR} of the ISR equilibrium orbit we must now find the relations between R^{e}_{PS} and R_{PS} and between R^{i}_{ISR} and R_{ISR}. We do this for the case of the present ISR beam without Terwilliger scheme.

It has been decided to eject this beam from an orbit which has a radial displacement

$$\Delta R = - 11.2 \text{ mm} \qquad (24)$$

over most of the circumference. A bump near the ejection septum magnet will increase the average radius a little such that

$$\overline{\Delta R} = - 7.7 \text{ mm} \qquad (25)$$

Thus we have:

$$R^{e}_{PS} = R_{PS} (1 - 7.7 \times 10^{-5}) \qquad (26)$$

The relation between the average radius of the injection orbit R^{i}_{ISR} and the equilibrium orbit radius R_{ISR} can be found as follows, anticipating orbit parameters which can only be calculated when the gradients are known. The radial position of the injection orbit at the kicker magnet

$$\Delta R_{KM} = - 44.5 \text{ mm} \qquad (27)$$

and the momentum compaction function α_{KM} there

$$\alpha_{KM} = 2.262 \text{ m} \qquad (28)$$

are known and allow us to calculate the momentum error of the injected beam:

$$\frac{\Delta p}{p} = \frac{\Delta R_{KM}}{\alpha_{KM}} = -0.0197 \qquad (29)$$

Knowing the transition energy $\gamma_t = 8.9685$[1] and its definition

$$\gamma_t = \left(\frac{\Delta R/R}{\Delta p/p}\right)^{\frac{1}{2}} \qquad (30)$$

directly allows to convert the momentum error into a change in circumference

$$\frac{\Delta R^i_{ISR}}{\Delta R_{ISR}} = -2.45 \times 10^{-4} \qquad (31)$$

Hence:

$$R^i_{ISR} = R_{ISR}\,(1 - 2.45 \times 10^{-4}) \qquad (32)$$

Combining (23), (26) and (32) and using $R_{PS} = 100$ m then yield the result:

$$R_{ISR} = 150.0253 \text{ m} \qquad (33)$$

$$C_{ISR} = 942.6368 \text{ m}$$

The physical lengths of the straight sections (Tab. 3) and of the magnet blocks (Tab. 1) were chosen such as to yield the circumference of the ISR equilibrium orbit given above.

The tolerance on the relation (23) between the PS and ISR radius is determined by the requirement that the bunches be well enough centered in the ISR buckets to limit the dilution in synchrotron phase space to a reasonable value. It turns out that this requirement is met when the PS ejection orbit radius is within ± 1 cm from the

correct value - as long as the transfer of all 20 bunches together is considered. The tolerance on the radius drops to about ± 1 mm for two-turn injection into the ISR, since then the number of RF cycles between the first and the last bunch in the ISR is much higher.

I.4.2 The shape of the ISR

The geometry of one ring of the ISR is uniquely determined by a polygon, which is formed by

i) the straight sections of the length L_s, and
ii) the magnet centre lines of the length L_n.

The bending angles define the angles of the polygon.

The second ring is obtained by rotating the first one by $\pi/4$.

The intersection radius, ρ_i = 148.6151 m, is the same for all intersection points, since a single ring exhibits a periodicity with the period $\pi/2$.

There is no machine radius with respect to which the rings have mirror symmetry due to the effect of the coil connections. Thus the corresponding distances from the intersection point to the neighbouring magnet are not equal.

The distances from the intersection point to the nearest magnet cores are given in Tab. 4.

Tab. 4

clockwise in the outer arc	6.9608 m
clockwise in the inner arc	9.8243 m
counterclockwise in the outer arc	6.9587 m
counterclockwise in the inner arc	9.8222 m

I.5 Gradient of ISR Magnets

All the effective focusing lengths of the ISR magnet blocks and of the straight sections are summarized in Tabs. 2 and 3. They were used to calculate - with the AGS program[2] - the gradients which yield the correct Q values.

Since the magnets are straight ones this option in the program was used. The result of the AGS program are two focusing parameters K_F and K_D which take the following values:

$$K_F = -0.03987\ m^{-2} \quad (34)$$

$$K_D = +0.03840\ m^{-2} \quad (35)$$

In order to obtain the profile parameters these values have to be multiplied by the bending radius ρ given in (18):

$$(n/\rho)_F = -3.133\ m^{-1} \quad (36)$$

$$(n/\rho)_D = +3.018\ m^{-1} \quad (37)$$

The Q values are made approximately independent of momentum by adding a quadratic variation with radius to the field of the ISR magnets. The sextupole component required to achieve this aim was also calculated by the AGS program. Again, the result is given in the form of radial derivatives of the focusing parameter

$$K'_F = -0.02469\ m^{-3} \quad (38)$$

$$K'_D = +0.01903\ m^{-3} \quad (39)$$

and must be transformed into derivatives of the profile parameter by multiplication with ρ:

$$(n'/\rho)_F = -1.940\ m^{-2} \quad (40)$$

$$(n'/\rho)_D = +1.496\ m^{-2} \quad (41)$$

The resulting variation of the Q values with the momentum error $\Delta p/p$ is shown in Tab. 5. The quadratic variation of the Q values with $\Delta p/p$ is to be expected in a magnet with a linear variation in gradient and a linear variation of the effective length across the aperture.

Tab. 5. Q values in the hard edge approximation

$\Delta p/p$	Q_H	Q_V
- 0.02	8.791	8.714
- 0.01	8.793	8.704
0	8.793	8.700
+ 0.01	8.793	8.703
+ 0.02	8.791	8.713

Part II. Tracking of Proton Orbits in the ISR

II.1 Introduction

This part describes the results of tracking proton orbits through the magnet structure of the ISR by direct numerical integration of the equations of motion[3].

This integration is based on a table of the magnetic field in the median plane of the ISR. Details about the field table are given in Chapter II.2.

The purpose of this work is to check the validity of the approximations made in the determination of the ISR geometry and of the magnet profile parameter by the hard-edge matrix method described in Part I. This aim is achieved by finding the closed orbits for a range of momenta, and by calculating the transfer matrices for small oscillations in their vicinity. The results on the closed orbit are given in Chapter II.3, those on the transfer matrices in Chapter II.4. Chapter II.5 summarizes the conclusions.

II.2 The Magnetic Field

II.2.1 Fieldtable

Since the field in the junction of two blocks forming a long magnet is quite different from the fringing field at the end, we have to deal with four different fieldtables (F-end, F-junction, D-end, D-junction). Connection end and free end of a magnet block were considered equal. The average fringe field was used in the fieldtable.

The coordinate system used in the median plane ($y = 0$) of a magnet block is shown in Fig. 1. $z = 0$ is in the middle of the block.

The field was given in terms of $B(x,o)/B(o,o)$ in the nodes of the mesh described by Tab. 5. The field is symmetrical to $z = 0$ in a short unit and vanishes at a distance of 0.5 m ($z = - 1.72$) from the end face of the magnet.

Tab. 5

Region	Step width	Magnet type
$-1.72 \leq z \leq -0.92$	$\Delta z = 0.02$	S,L
$-0.92 \leq z \leq 0$	constant field	S,L
$0 \leq z \leq +0.995$	constant field	L
$+1.095 \leq z \leq +0.995$	$\Delta z = 0.02$	L
$+1.345 \leq z \leq +1.095$	$\Delta z = 0.01$	L
$-0.06 \leq x \leq 0.06$	$\Delta x = 0.01$	S,L
$0.06 \leq \lvert x \rvert \leq 0.42$	$\Delta x = 0.02$	S,L

All lengths in m.

At the time when the fieldtable was established only a magnet model existed which did not have exactly the same profile and effective lengths as the final ISR magnets.

Therefore a slight adjustment was necessary in order to arrive at a field table which had exactly the same overall properties as the field of the final ISR magnets.

The change in the profile was taken into account by multiplying $B_1(x,z)$ by $B_2(x,o)/B_1(x,o)$, the ratio of the new field to the old field at $z = 0$ calculated from the gradients.

The effective length was changed by performing the transformation

$$B_3(x,z) = B_2(x,z + \delta L_B(x))$$

where B_2 is the result of the first transformation and B_3 the result of the second one.

II.2.2 The interpolation in the fieldtable

The interpolation in the x-direction was done by means of a parabola fitted to the field in 9 points which were disposed symmetrical to the x-axis. The step width between two points was 0.01 m. This was done for every z-coordinate where the field was specified.

It was made sure afterwards that the orbits are within $-0.05 < x < 0.05$. Although the field at $x = \pm 0.05$ m was not included in the fit, one can be fairly sure that the approximation is still good in the region $0.05 > |x| > 0.04$.

Linear interpolation was used in the z-direction.

II.3 The Closed Orbits

The geometry of the ISR was established by the hard-edge method.

The central orbit in this approximation does not precisely correspond to a real proton orbit. One of the aims of this investigation was to find that real proton orbit - and the momentum of the protons - which comes closest to the central orbit, defined in Part I as the orbit coinciding outside the magnetic field with a line g defined in every straight section. The relative position of this line can be seen in Fig. 1.

"Closest" was interpreted in the way that this real proton orbit should have the same maximum positive and negative deviation from the lines g over an octant.

The question arises: why is it not possible to have an orbit coinciding with the lines g? The answer is that the trajectory for a particle of a certain momentum does not leave the magnetic field at the same x in all four types of the magnets if one wants to retain the bending angles given by the hard edge method.

This can be seen from the following argument. The equations of motion in the median plane of a magnet are:

$$\frac{d^2x}{dt^2} = -\frac{dz}{dt} B \frac{e}{mc}$$
$$\frac{d^2z}{dt^2} = \frac{dx}{dt} B \frac{e}{mc} \qquad (1)$$

Or

$$\frac{dx}{dt} = u$$
$$\frac{dz}{dt} = v$$
$$\frac{du}{dt} = -v\, B(x,z) \frac{e}{cm} \qquad (2)$$
$$\frac{dv}{dt} = u\, B(x,z) \frac{e}{cm}$$

The solutions of this system of differential equations are:

$$
\begin{aligned}
x &= g_1 (C_i, t) \\
z &= g_2 (C_i, t) \\
\frac{dx}{dt} &= h_1 (C_i, t) \\
\frac{dz}{dt} &= h_2 (C_i, t)
\end{aligned}
\qquad (3)
$$

The C_i, $i = 1,2,3,4$ are constants determined by the conditions one imposes on the solutions. One of the constants is determined by $z(t = 0) = z_o$, which can be chosen arbitrarily. Then we are left with three constants.

A solution of the equations (3) can be found for magnet 1, being someone or other of the 4 types of magnets, which fulfils

i) symmetry to the vertical symmetry plane of the magnet (not of the magnet block);
ii) bending angle;
iii) x shall have a certain value at the exit of the field.

The trajectory is fixed uniquely by these conditions, therefore also the momentum p of the particle, which shall be equal for all magnets. Thus for the remaining magnets we can maintain only two of the above conditions, p being the third one.

If one does not want to touch i) and if one wants to keep the bending angles, evaluated by the hard-edge method, iii) will no longer hold for the 3 magnets left, since the bending angles were calculated by the hard-edge method which assumes the same shape of the trajectory for all magnets. In reality the trajectory will have a different shape in different types of magnets: e.g. the D-magnet bends more at the ends

and less in the middle than the F-magnet. Thus the trajectory in these magnets will leave them at the wanted angle, i.e. parallel to the straight section, but with a displacement x different for every magnet.

The next question one may ask is: how much is this difference in the exit coordinate at the border of the hard-edge field?

Table II shows the result of a tracking procedure where the approach described above was used. LD was chosen to be the magnet 1 and the third condition had the form

$$x(z = L_n/2 + \ell_B) = 0.0072 \text{ m}.$$

The momentum $p = m_o \gamma v$ turned out to be 23.585 GeV/c.

Table II

	a [mm]	b [mm]	a+b [mm]
SF	6.72	3.98	10.70
SD	7.38	3.20	10.58
LF	6.59	3.85	10.44
LD	7.20	3.14	10.34

$b = x(z = 0)$; $a = x(z = L_n/2 + \ell_B)$.

a + b is larger for F-magnets since the curvature increases towards the middle of the magnet whereas a D-magnet bends more at the ends. Further one can see that the a values are different, which proves the argument put forward above.

There are now two ways of proceeding. Either we change the bending angles in order to get equal a's in all magnets, or we accept a closed

orbit whose maximum deviation from the lines g would probably be of the same magnitude as the difference in the values of a. Since the former alternative would have involved a rearrangement of the ISR geometry, and since the difference in a turned out to be rather small, the latter alternative was chosen.

At a field level of 1T, the orbit of a particle with p = 23.558 GeV/c turned out to be closest to the central orbit defined before. Henceforth we refer to this orbit as the orbit with $\Delta p/p = 0$.

Figure 2 shows the displacement of this orbit from the lines g_i in the straight sections of an octant. It is sufficient to consider an octant since we did not take into account the influence of the coil connections onto the magnetic field.

The maximum deviation from the lines g_i is ~ 0.4 mm, as expected, which is small compared to the horizontal closed orbit distortions, which are assumed to be about 15 mm[1].

Figures 3 and 4 show this deviation for the orbits with $\Delta p/p = \pm 0.02$ and compares it with the result of the hard-edge method. The agreement is satisfactory.

II.4 The Q-values

As far as the numerical methods used to calculate the transfer matrices are concerned, the reader is referred to [3].

The result of the computations is shown in Table III and Fig. 5.

Table III

$\Delta p/p$	-0.02	-0.01	0.00	+0.01	+0.02
Q_H	8.779	8.781	8.781	8.781	8.781
Q_V	8.667	8.671	8.677	8.686	8.694

$\Delta p/p = 0 \equiv p = 23.558$ GeV/c.

The agreement with the values, given in Part I and shown in Fig. 6, is quite good, $\Delta Q/Q$ being less than $\sim 5 \cdot 10^{-3}$. To prove this was the second objective of this work.

The Q-values turned out to be extremely sensitive to the interpolation procedure. Thus the difference in the Q-values reflects mainly this difficulty.

II.5 Conclusions

It was shown by a numerical integration of the equations of motion that a closed orbit can be found in the ISR, which does not deviate more than ± 0.4 mm from the orbit found by the hard-edge approximation.

The computations were based on a fieldtable, which was derived from measurements on a prototype magnet at a field level of 0.5 T.

The Q-values derived from the numerically evaluated transfer matrices were found to be in agreement with those Q-values evaluated by the hard-edge model, the difference being

$$\frac{\Delta Q_V}{Q_V} \leq 5 \cdot 10^{-3} ,$$

$$\frac{\Delta Q_H}{Q_H} \leq 10^{-3} .$$

Acknowledgement

We are indebted to R. Keyser, who adapted the tracking program for the ISR.

References

1) ISR Parameter List (Revision 4), ISR-TH/68-32, 1968.

2) E. Keil and P. Strolin, CERN Yellow Report to be published.

3) R. Keyser, Particle Trajectories in the C.P.S. Magnetic Field computed by a Fortran Program, DD/CO/63/2, October 1963.

Figure Captions

Fig. 1 The relative position of the straight sections, the central orbit and the reference lines g.

Fig. 2 The displacement of the orbit $\Delta p/p = 0$ from the lines g in one octant. The scale in the different straight sections is chosen to give the same length for all.

Fig. 3 The displacement of the orbit $\Delta p/p = 0.02$ relative to g in the mid-points of the straight sections in one octant

. hard-edge method

x tracking

Fig. 4 Corresponds to Fig. 3 but for $\Delta p/p = - 0.02$.

Fig. 5 Q_H, Q_V-diagram. The numbers at the points of confluence of the resonance lines give the order of the resonances.
The rectangle enclosing the calculated Q-values shows the tolerances on the Q-values ("bullet-size").
The numbers next to the points correspond to the momentum spread in percent.

• hard-edge method

x tracking program.

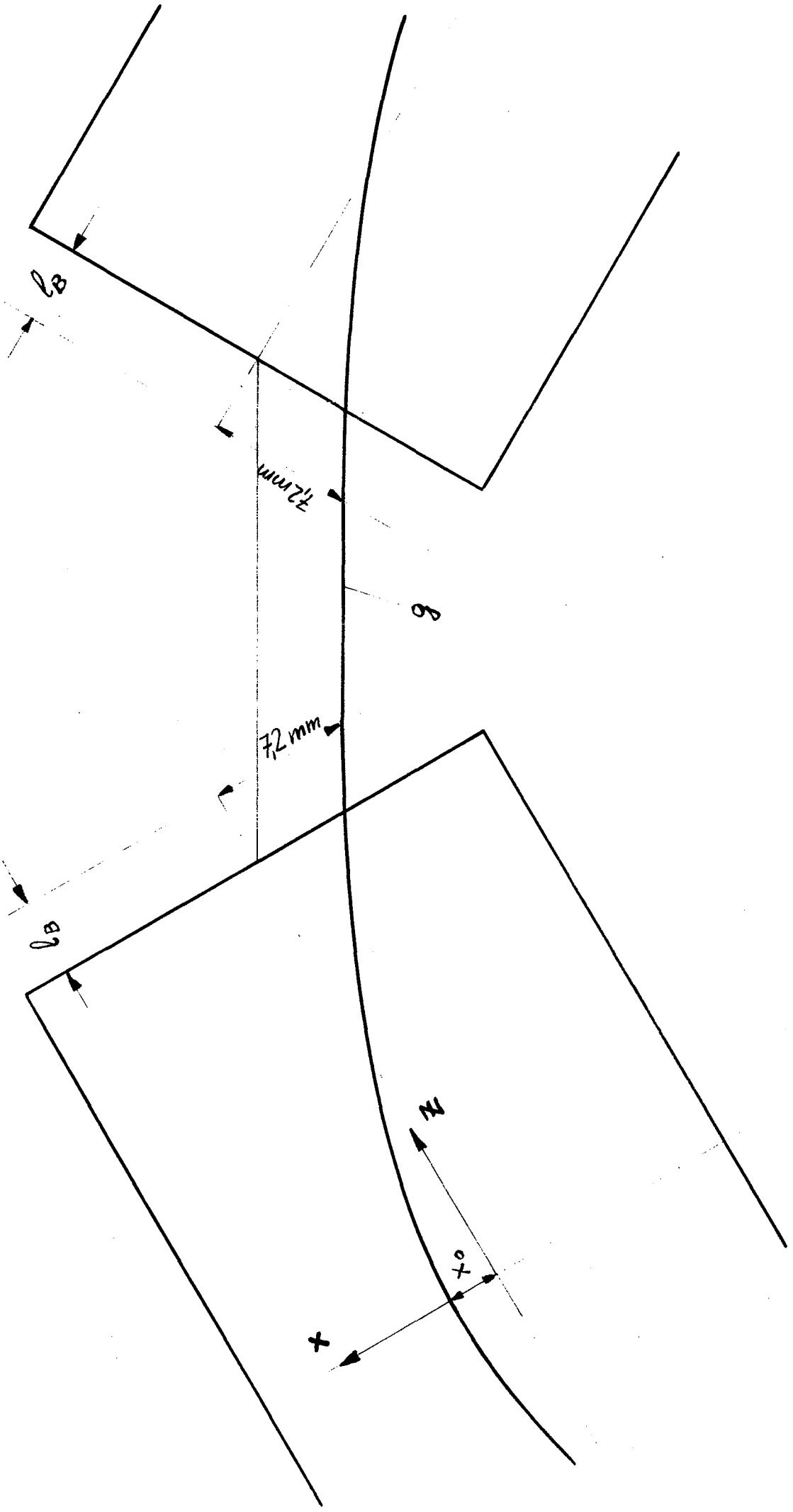

Fig. 1

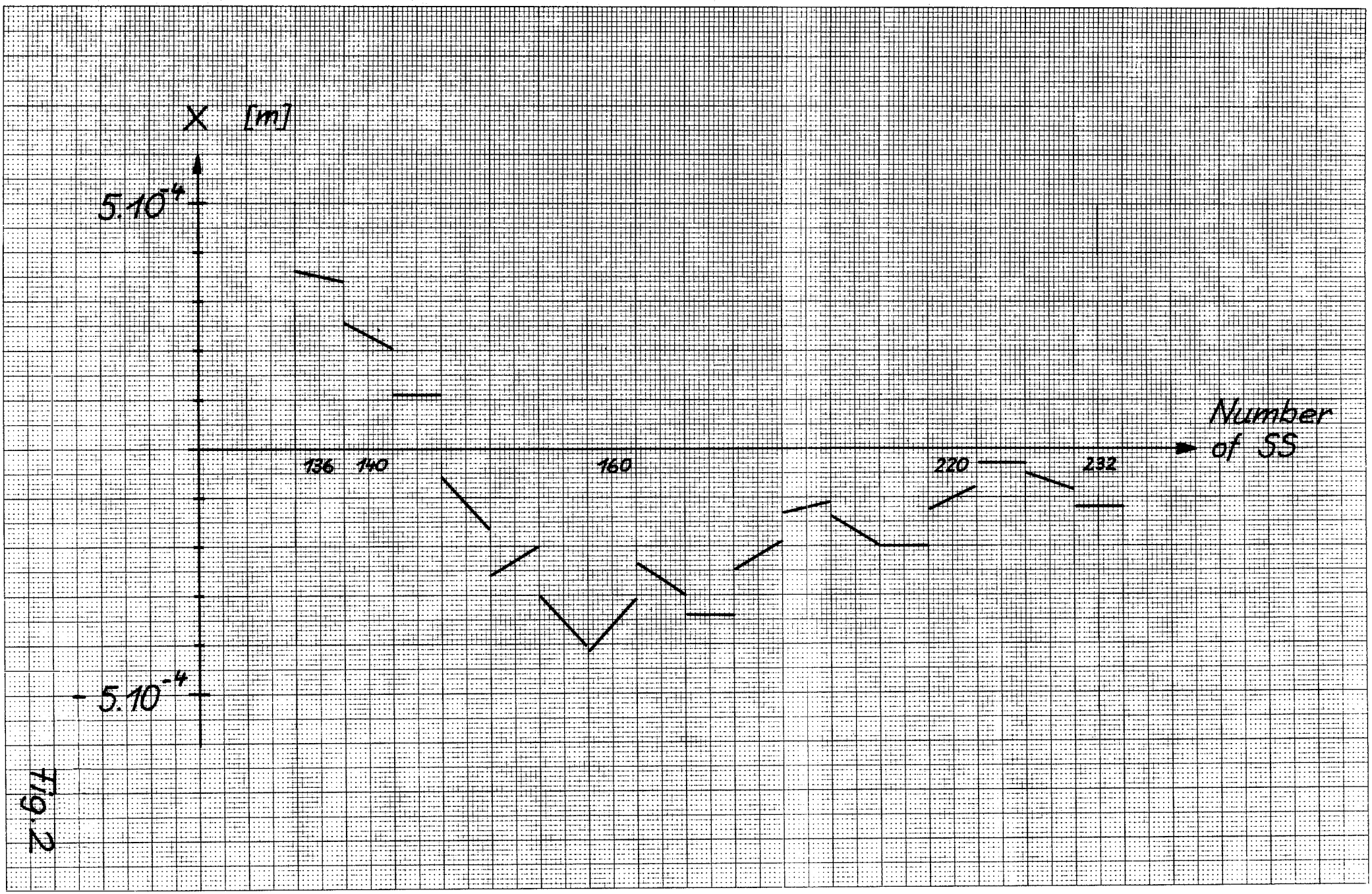

Fig. 2

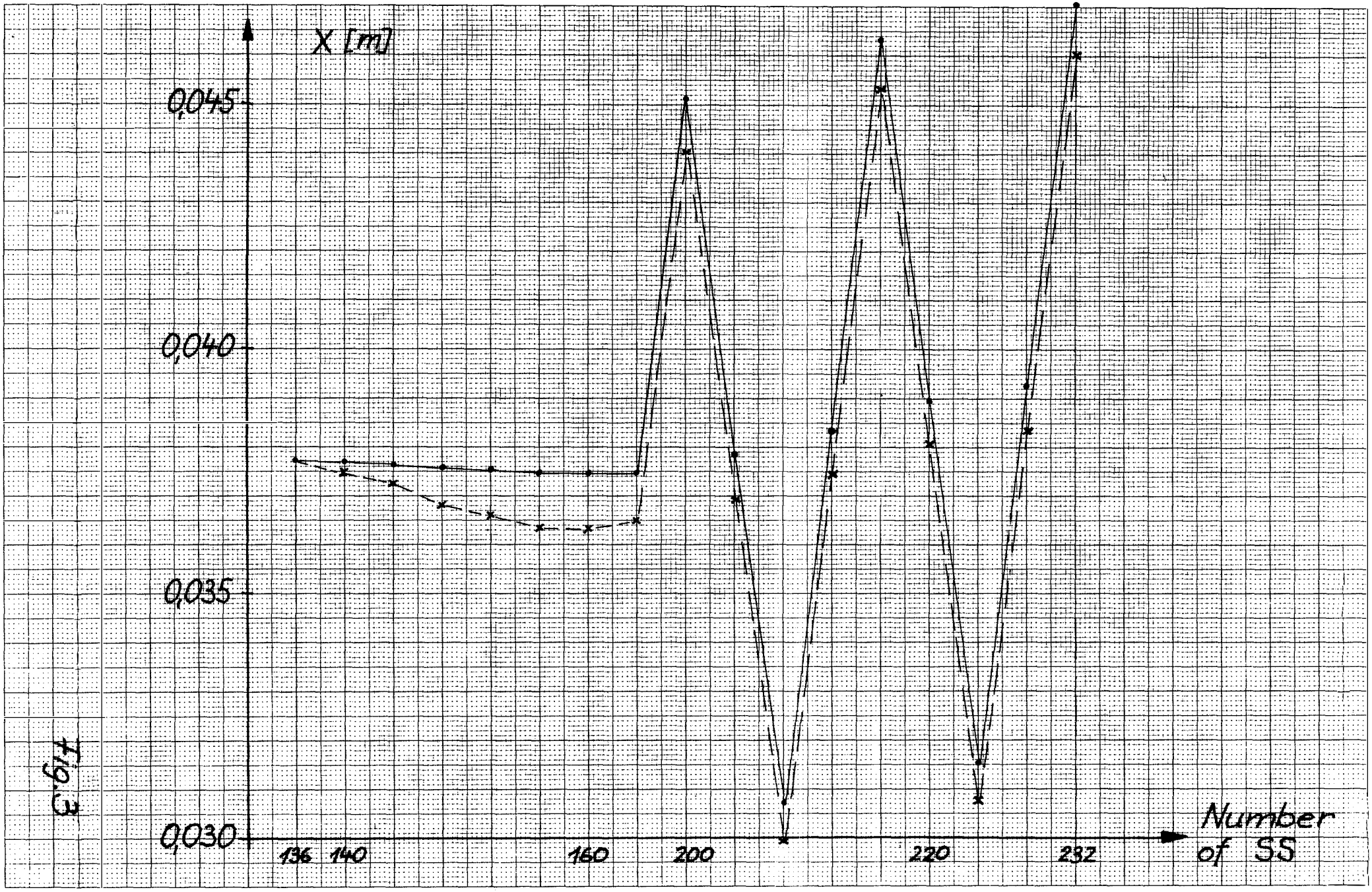

Fig. 3

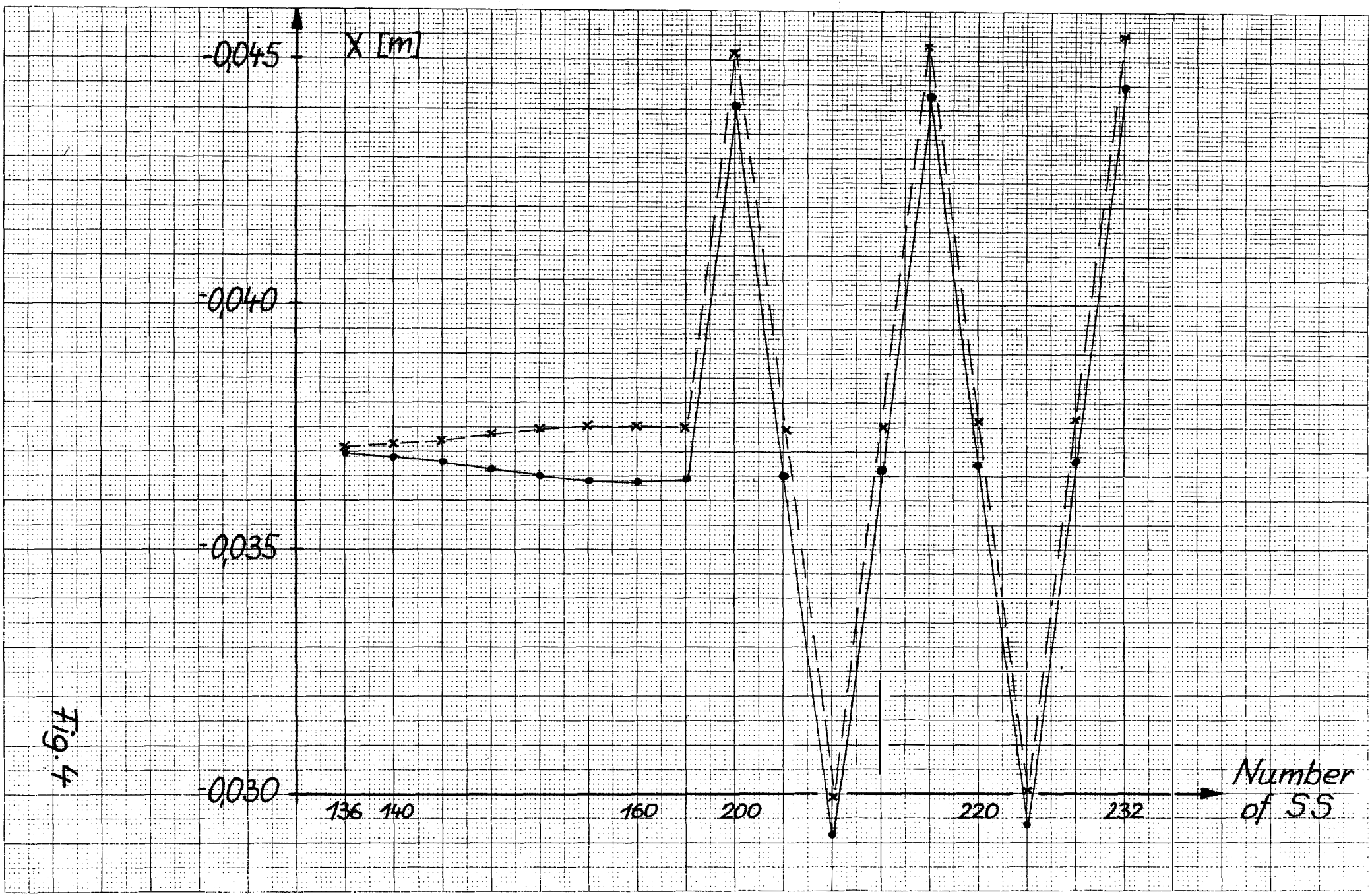

Fig. 4

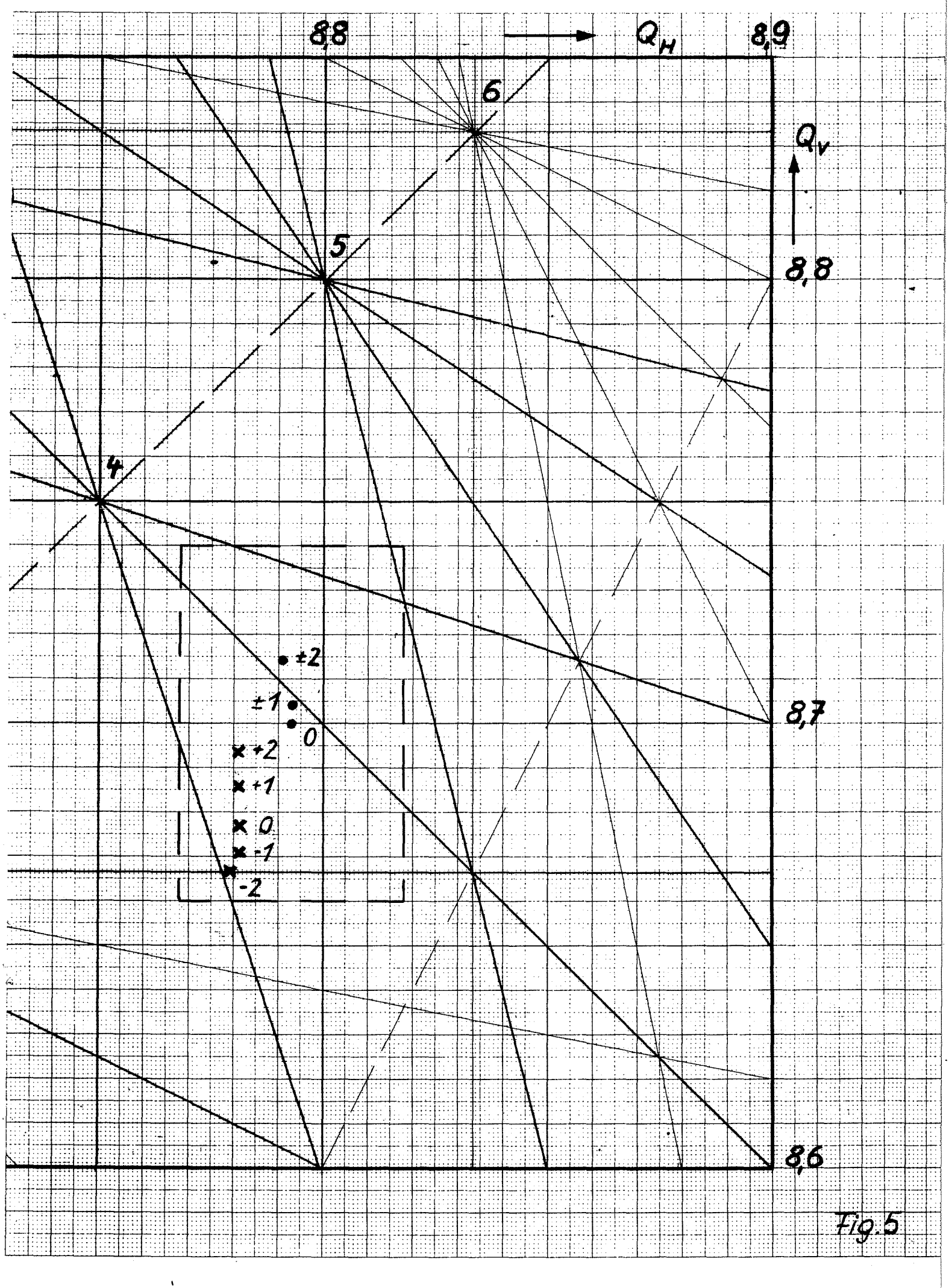

Fig. 5